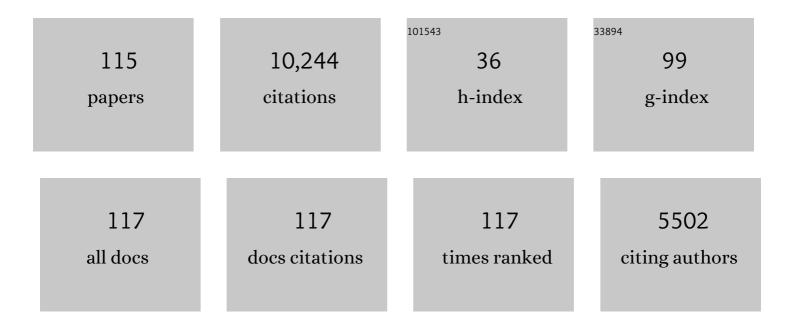
Anton Hohenwarter

List of Publications by Year in descending order

Source: https://exaly.com/author-pdf/2311954/publications.pdf Version: 2024-02-01



#	Article	IF	CITATIONS
1	A fracture-resistant high-entropy alloy for cryogenic applications. Science, 2014, 345, 1153-1158.	12.6	3,982
2	Exceptional damage-tolerance of a medium-entropy alloy CrCoNi at cryogenic temperatures. Nature Communications, 2016, 7, 10602.	12.8	1,175
3	Mechanical properties, microstructure and thermal stability of a nanocrystalline CoCrFeMnNi high-entropy alloy after severe plastic deformation. Acta Materialia, 2015, 96, 258-268.	7.9	952
4	Saturation of Fragmentation During Severe Plastic Deformation. Annual Review of Materials Research, 2010, 40, 319-343.	9.3	460
5	Fatigue crack closure: a review of the physical phenomena. Fatigue and Fracture of Engineering Materials and Structures, 2017, 40, 471-495.	3.4	225
6	Nanomaterials by severe plastic deformation: review of historical developments and recent advances. Materials Research Letters, 2022, 10, 163-256.	8.7	215
7	Thermodynamic instability of a nanocrystalline, single-phase TiZrNbHfTa alloy and its impact on the mechanical properties. Acta Materialia, 2018, 142, 201-212.	7.9	196
8	Effect of temperature on the fatigue-crack growth behavior of the high-entropy alloy CrMnFeCoNi. Intermetallics, 2017, 88, 65-72.	3.9	160
9	Technical parameters affecting grain refinement by high pressure torsion. International Journal of Materials Research, 2009, 100, 1653-1661.	0.3	159
10	Advantages and Limitations of HPT: A Review. Materials Science Forum, 0, 584-586, 16-21.	0.3	115
11	The use of femtosecond laser ablation as a novel tool for rapid micro-mechanical sample preparation. Materials and Design, 2017, 121, 109-118.	7.0	92
12	Increasing the strength of nanocrystalline steels by annealing: Is segregation necessary?. Scripta Materialia, 2015, 95, 27-30.	5.2	89
13	The importance of fracture toughness in ultrafine and nanocrystalline bulk materials. Materials Research Letters, 2016, 4, 127-136.	8.7	82
14	Anisotropic deformation characteristics of an ultrafine- and nanolamellar pearlitic steel. Acta Materialia, 2016, 106, 239-248.	7.9	82
15	Fracture toughness evaluation of ultrafine-grained nickel. Scripta Materialia, 2011, 64, 982-985.	5.2	80
16	New procedure to generate stable nanocrystallites by severe plastic deformation. Scripta Materialia, 2009, 61, 1016-1019.	5.2	74
17	Effect of Large Shear Deformations on the Fracture Behavior of a Fully Pearlitic Steel. Metallurgical and Materials Transactions A: Physical Metallurgy and Materials Science, 2011, 42, 1609-1618.	2.2	72
18	Nearâ€threshold behaviour of shearâ€mode fatigue cracks in metallic materials. Fatigue and Fracture of Engineering Materials and Structures, 2014, 37, 232-254.	3.4	68

#	Article	IF	CITATIONS
19	Nanoindentation testing as a powerful screening tool for assessing phase stability of nanocrystalline high-entropy alloys. Materials and Design, 2017, 115, 479-485.	7.0	68
20	Incremental high pressure torsion as a novel severe plastic deformation process: Processing features and application to copper. Materials Science & Engineering A: Structural Materials: Properties, Microstructure and Processing, 2015, 626, 80-85.	5.6	67
21	Anisotropic fracture behavior of ultrafine-grained iron. Materials Science & Engineering A: Structural Materials: Properties, Microstructure and Processing, 2010, 527, 2649-2656.	5.6	64
22	Fracture of ECAP-deformed iron and the role of extrinsic toughening mechanisms. Acta Materialia, 2013, 61, 2973-2983.	7.9	60
23	Fracture and fracture toughness of nanopolycrystalline metals produced by severe plastic deformation. Philosophical Transactions Series A, Mathematical, Physical, and Engineering Sciences, 2015, 373, 20140366.	3.4	60
24	Tailoring bimodal grain size structures in nanocrystalline compositionally complex alloys to improve ductility. Materials Science & Engineering A: Structural Materials: Properties, Microstructure and Processing, 2019, 748, 379-385.	5.6	54
25	Direct evidence for grain boundary motion as the dominant restoration mechanism in the steady-state regime of extremely cold-rolled copper. Acta Materialia, 2014, 77, 401-410.	7.9	52
26	Grain boundary excess volume and defect annealing of copper after high-pressure torsion. Acta Materialia, 2014, 68, 189-195.	7.9	51
27	Thermally activated deformation processes in body-centered cubic Cr – How microstructure influences strain-rate sensitivity. Scripta Materialia, 2015, 106, 42-45.	5.2	50
28	Ultra-strong and damage tolerant metallic bulk materials: A lesson from nanostructured pearlitic steel wires. Scientific Reports, 2016, 6, 33228.	3.3	49
29	Influence of Annealing on Microstructure and Mechanical Properties of a Nanocrystalline CrCoNi Medium-Entropy Alloy. Materials, 2018, 11, 662.	2.9	48
30	Medium-range order dictates local hardness in bulk metallic glasses. Materials Today, 2021, 44, 48-57.	14.2	47
31	The ductile to brittle transition of ultrafine-grained Armco iron: an experimental study. Journal of Materials Science, 2010, 45, 4805-4812.	3.7	45
32	Enhanced fatigue endurance of metallic glasses through a staircase-like fracture mechanism. Proceedings of the National Academy of Sciences of the United States of America, 2013, 110, 18419-18424.	7.1	43
33	Microstructure and metallic ion release of pure titanium and Ti–13Nb–13Zr alloy processed by high pressure torsion. Materials and Design, 2016, 91, 340-347.	7.0	43
34	Revisiting fatigue crack growth in various grain size regimes of Ni. Materials Science & Engineering A: Structural Materials: Properties, Microstructure and Processing, 2015, 646, 294-305.	5.6	41
35	A comprehensive study on the damage tolerance of ultrafine-grained copper. Materials Science & Engineering A: Structural Materials: Properties, Microstructure and Processing, 2012, 540, 89-96.	5.6	40
36	Insights into the deformation behavior of the CrMnFeCoNi high-entropy alloy revealed by elevated temperature nanoindentation. Journal of Materials Research, 2017, 32, 2658-2667.	2.6	40

#	Article	IF	CITATIONS
37	Strain effects on the coarsening and softening of electrodeposited nanocrystalline Ni subjected to high pressure torsion. Scripta Materialia, 2008, 58, 790-793.	5.2	39
38	Microstructure, Texture, and Strength Development during High-Pressure Torsion of CrMnFeCoNi High-Entropy Alloy. Crystals, 2020, 10, 336.	2.2	39
39	Phase Decomposition of a Singleâ€Phase AlTiVNb Highâ€Entropy Alloy after Severe Plastic Deformation and Annealing. Advanced Engineering Materials, 2017, 19, 1600674.	3.5	36
40	Influence of morphology and structural size on the fracture behavior of a nanostructured pearlitic steel. Materials Science & Engineering A: Structural Materials: Properties, Microstructure and Processing, 2013, 585, 190-196.	5.6	35
41	On the Room-Temperature Mechanical Properties of an Ion-Irradiated TiZrNbHfTa Refractory High Entropy Alloy. Jom, 2020, 72, 130-138.	1.9	34
42	Fatigue crack growth anisotropy in ultrafine-grained iron. Acta Materialia, 2017, 126, 154-165.	7.9	33
43	Influence of grain shape and orientation on the mechanical properties of high pressure torsion deformed nickel. Materials Science & Engineering A: Structural Materials: Properties, Microstructure and Processing, 2013, 560, 224-231.	5.6	32
44	Near-threshold propagation of mode II and mode III fatigue cracks in ferrite and austenite. Acta Materialia, 2013, 61, 4625-4635.	7.9	30
45	Influence of severe plastic deformation and specimen orientation on the fatigue crack propagation behavior of a pearlitic steel. Materials Science & Engineering A: Structural Materials: Properties, Microstructure and Processing, 2018, 710, 260-270.	5.6	27
46	Microstructure and texture evolution during severe plastic deformation of CrMnFeCoNi high-entropy alloy. IOP Conference Series: Materials Science and Engineering, 2017, 194, 012028.	0.6	24
47	Analysis of fatigue crack propagation under mixed mode II+III in ARMCO iron. International Journal of Fatigue, 2015, 76, 47-52.	5.7	22
48	The effect of severe grain refinement on the damage tolerance of a superelastic NiTi shape memory alloy. Journal of the Mechanical Behavior of Biomedical Materials, 2017, 71, 337-348.	3.1	22
49	Influence of testing orientation on mechanical properties of Ti45Nb deformed by high pressure torsion. Materials and Design, 2017, 114, 40-46.	7.0	22
50	On the onset of deformation twinning in the CrFeMnCoNi high-entropy alloy using a novel tensile specimen geometry. Intermetallics, 2019, 110, 106469.	3.9	21
51	Three-dimensional morphology of fracture surfaces generated by modes II and III fatigue loading in ferrite and austenite. Engineering Fracture Mechanics, 2013, 108, 285-293.	4.3	20
52	Gradient residual strain and stress distributions in a high pressure torsion deformed iron disk revealed by high energy X-ray diffraction. Scripta Materialia, 2018, 146, 178-181.	5.2	20
53	Microstructure-dependent phase stability and precipitation kinetics in equiatomic CrMnFeCoNi high-entropy alloy: Role of grain boundaries. Acta Materialia, 2022, 223, 117470.	7.9	20
54	Simultaneous enhancement of strength and fatigue crack growth behavior of nanocrystalline steels by annealing. Scripta Materialia, 2017, 139, 39-43.	5.2	19

#	Article	IF	CITATIONS
55	Effect of processing temperature on the microstructural characteristics of Cu-Ag nanocomposites: From supersaturation to complete phase decomposition. Acta Materialia, 2018, 154, 33-44.	7.9	19
56	Influence of annealing on microstructure and mechanical properties of ultrafine-grained Ti45Nb. Materials and Design, 2019, 179, 107864.	7.0	19
57	Cyclic Deformation Behavior of a 316L Austenitic Stainless Steel Processed by High Pressure Torsion. Advanced Engineering Materials, 2012, 14, 948-954.	3.5	18
58	Hardening by annealing: insights from different alloys. IOP Conference Series: Materials Science and Engineering, 2015, 89, 012043.	0.6	18
59	Sample Size and Strain-Rate-Sensitivity Effects on the Homogeneity of High-Pressure Torsion Deformed Disks. Metallurgical and Materials Transactions A: Physical Metallurgy and Materials Science, 2019, 50, 601-608.	2.2	18
60	Experimental evidence of a common local mode II growth mechanism of fatigue cracks loaded in modes II, III and II + III in niobium and titanium. International Journal of Fatigue, 2016, 92, 470-477.	5.7	17
61	Evaluation of the intergranular crack growth resistance of ultrafine grained tungsten materials. Acta Materialia, 2019, 176, 330-340.	7.9	17
62	Direct measurement of vacancy relaxation by dilatometry. Applied Physics Letters, 2016, 109, .	3.3	16
63	Femtosecond laser machining for characterization of local mechanical properties of biomaterials: a case study on wood. Science and Technology of Advanced Materials, 2017, 18, 574-583.	6.1	16
64	Impact of severe plastic deformation on microstructure and fracture toughness evolution of a duplex-steel. Materials Science & Engineering A: Structural Materials: Properties, Microstructure and Processing, 2017, 703, 173-179.	5.6	16
65	Precipitation behavior of a Co-free Fe-Ni-Cr-Mo-Ti-Al maraging steel after severe plastic deformation. Materials Science & Engineering A: Structural Materials: Properties, Microstructure and Processing, 2022, 833, 142416.	5.6	15
66	Ultimate Strength of a Tungsten Heavy Alloy after Severe Plastic Deformation at Quasi-Static and Dynamic Loading. Materials Science Forum, 0, 584-586, 405-410.	0.3	14
67	Influence of heat treatment on the microstructural evolution of Al–3 wt.% Cu during high-pressure torsion. Philosophical Magazine Letters, 2014, 94, 342-350.	1.2	14
68	Progress in understanding of intrinsic resistance to shear-mode fatigue crack growth in metallic materials. International Journal of Fatigue, 2016, 89, 36-42.	5.7	14
69	Fracture properties of ultrafine grain chromium correlated to single dislocation processes at room temperature. Journal of Materials Research, 2019, 34, 2370-2383.	2.6	14
70	Anisotropy in fracture and fatigue resistance of pearlitic steels and its effect on the crack path. International Journal of Fatigue, 2019, 124, 528-536.	5.7	14
71	Electrochemical and biocompatibility examinations of highâ€pressure torsion processed titanium and T i–13 N b–13 Z r alloy. Journal of Biomedical Materials Research - Part B Applied Biomaterials, 2018, 106, 1097-1107.	3.4	13
72	Crack path identification in a nanostructured pearlitic steel using atom probe tomography. Scripta Materialia, 2018, 142, 66-69.	5.2	13

#	Article	IF	CITATIONS
73	Microstructures, Mechanical Properties, and Corrosion Behaviors of Refractory High-Entropy ReTaWNbMo Alloys. Journal of Materials Engineering and Performance, 2020, 29, 399-409.	2.5	13
74	An SEM compatible plasma cell for <i>in situ</i> studies of hydrogen-material interaction. Review of Scientific Instruments, 2020, 91, 043705.	1.3	13
75	Deformation and fracture characteristics of ultrafine-grained vanadium. Materials Science & Engineering A: Structural Materials: Properties, Microstructure and Processing, 2016, 650, 492-496.	5.6	12
76	Introduction of Planar High Pressure Torsion (Pâ€HPT) for Fabrication of Nanostructured Sheets. Advanced Engineering Materials, 2018, 20, 1800050.	3.5	12
77	High pressure torsion processing of maraging steel 250: Microstructure and mechanical behaviour evolution. Materials Science & Engineering A: Structural Materials: Properties, Microstructure and Processing, 2021, 802, 140665.	5.6	12
78	A novel laboratory test rig for probing the sensitivity of rail steels to RCF and wear – first experimental results. Wear, 2014, 316, 101-108.	3.1	11
79	Anisotropy of Tensile and Fracture Behavior of Pure Titanium after Hydrostatic Extrusion. Materials Transactions, 2019, 60, 2160-2167.	1.2	11
80	Grain refinement effect on the Ti-45Nb alloy electrochemical behavior in simulated physiological solution. Surface and Coatings Technology, 2021, 423, 127609.	4.8	11
81	Influence of cold rolling on the fatigue crack growth behavior of tungsten. Materials Science & Engineering A: Structural Materials: Properties, Microstructure and Processing, 2021, 805, 140791.	5.6	10
82	The Role of Phase Hardness Differential on the Non-uniform Elongation of a Ferrite-Martensite Dual Phase Steel. Metallurgical and Materials Transactions A: Physical Metallurgy and Materials Science, 2021, 52, 4018-4032.	2.2	10
83	Prediction of effective mode II fatigue crack growth threshold for metallic materials. Engineering Fracture Mechanics, 2017, 174, 117-126.	4.3	9
84	Optimizing mechanical properties of Fe26.7Co26.7Ni26.7Si8.9B11 high entropy alloy by inducing hypoeutectic to quasi-duplex microstructural transition. Scientific Reports, 2019, 9, 360.	3.3	9
85	Quasi-static and dynamic fracture toughness of a γ-TiAl alloy: Measurement techniques, fractography and interpretation. Engineering Fracture Mechanics, 2021, 258, 108081.	4.3	9
86	Structural anisotropy in equal-channel angular extruded nickel revealed by dilatometric study of excess volume. International Journal of Materials Research, 2017, 108, 81-88.	0.3	8
87	Mechanical Behavior and In Vitro Corrosion of Cubic Scaffolds of Pure Magnesium Processed by Severe Plastic Deformation. Metals, 2021, 11, 1791.	2.3	8
88	Fatigue Crack Growth Behavior of Ultrafine-grained Nickel Produced by High Pressure Torsion. , 2014, 3, 1044-1049.		7
89	Electron Irradiation Effects on Strength and Ductility of Polymer Foils Studied by Femtosecond Laser-Processed Micro-Tensile Specimens. Materials, 2019, 12, 1468.	2.9	7
90	Corrosion in Hank's Solution and Mechanical Strength of Ultrafineâ€Grained Pure Iron. Advanced Engineering Materials, 2020, 22, 2000183.	3.5	7

#	Article	IF	CITATIONS
91	Extracting information from noisy data: strain mapping during dynamic in situ SEM experiments. Journal of Materials Research, 2021, 36, 2291-2304.	2.6	7
92	Fracture of severely plastically deformed Ta and Nb. International Journal of Refractory Metals and Hard Materials, 2017, 64, 143-150.	3.8	6
93	Strength and ductility of heavily deformed pearlitic microstructures. IOP Conference Series: Materials Science and Engineering, 2017, 219, 012003.	0.6	6
94	Achieving 1 GPa fatigue strength in nanocrystalline 316L steel through recovery annealing. Scripta Materialia, 2022, 217, 114773.	5.2	6
95	An Overview on the Fracture Behavior of Metals Processed by High Pressure Torsion. Materials Science Forum, 2010, 667-669, 671-676.	0.3	4
96	The corrosion resistance in artificial saliva of titanium and Ti-13Nb-13Zr alloy processed by high pressure torsion. Procedia Structural Integrity, 2018, 13, 1834-1839.	0.8	4
97	Microstructure, strength and fracture toughness of CuNb nanocomposites processed with high pressure torsion using multi-sector disks. Scripta Materialia, 2020, 189, 48-52.	5.2	4
98	Influence of grain aspect-ratio on the fracture properties of ultrafine-grained tantalum. Materials and Design, 2022, 216, 110545.	7.0	4
99	Deformation-induced medium-range order changes in bulk metallic glasses. Physical Review Materials, 2022, 6, .	2.4	4
100	Crack path investigations in a pearlitic rail steel after pre-deformation under cyclic Mode-II loading. Engineering Failure Analysis, 2022, 140, 106567.	4.0	4
101	3D Morphology of Fracture Surfaces Created by Mixed-mode II+III Fatigue Loading in Metallic Materials. Procedia Engineering, 2014, 74, 74-77.	1.2	3
102	Internal stress and defect-related free volume in submicrocrystalline Ni studied by neutron diffraction and difference dilatometry. Philosophical Magazine Letters, 2017, 97, 450-458.	1.2	3
103	Influence of Secondary Phase on Intrinsic Threshold and Path of Shear-Mode Fatigue Cracks in Metals. Acta Physica Polonica A, 2018, 134, 699-702.	O.5	3
104	Load history effects on fatigue crack propagation: Its effect on the R-curve for threshold. Frattura Ed Integrita Strutturale, 2015, 9, 209-214.	0.9	3
105	Fatigue crack growth of deformed pearlitic rail steels under multiaxial loading. Procedia Structural Integrity, 2022, 39, 313-326.	0.8	3
106	Soft Magnetic Properties of Ultra-Strong and Nanocrystalline Pearlitic Wires. Nanomaterials, 2022, 12, 23.	4.1	3
107	Microstructural Impact on Fatigue Crack Growth Behavior of Alloy 718. Metals, 2022, 12, 710.	2.3	3
108	Microstructure and Failure Characteristics of Nanostructured Molybdenum–Copper Composites. Advanced Engineering Materials, 2020, 22, 1900474.	3.5	2

#	Article	IF	CITATIONS
109	The beneficial effect of rolling on the fracture toughness and R-curve behavior of pure tungsten. Materials Science & Engineering A: Structural Materials: Properties, Microstructure and Processing, 2022, 838, 142756.	5.6	2
110	Effects of microstructure and crystallography on crack path and intrinsic resistance to shear-mode fatigue crack growth. Frattura Ed Integrita Strutturale, 2015, 9, .	0.9	1
111	Fatigue Crack-Growth Properties of SPD-Metals. Structural Integrity, 2019, , 347-349.	1.4	1
112	Fracture of severely plastically deformed titanium. Materials Letters, 2021, 309, 131382.	2.6	1
113	Effect of a single overload on the cyclic R-curve behaviour of a Î ³ -TiAl TNM alloy. International Journal of Fatigue, 2022, 163, 107083.	5.7	1
114	Nanostructured Metallic Materials and Composites: Processes, Properties and Microstructures. Advanced Engineering Materials, 2019, 21, 1801073.	3.5	0
115	Propagation of Long Fatigue Cracks under Remote Modes II and III in Ferritic-Pearlitic Steel. Acta Physica Polonica A, 2015, 128, 611-614.	0.5	0